COMPARISON OF EXPERIMENTAL DATA TO THE RELATIVISTIC QUANTUM MOLECULAR DYNAMICS MODEL FOR Si+Au COLLISIONS AT 14.6 A GeV/c

M. GONIN[a], OLE HANSEN[b], B. MOSKOWITZ, and F. VIDEBÆK

Department of Physics, Brookhaven National Laboratory, Upton, NY 11973, U.S.A.

H. SORGE[c]

Theory Division, Los Alamos National Laboratory, Los Alamos, NM 87544, U.S.A.

R. MATTIELLO

Institut für Theoretische Physik, Johann Wolfgang Goethe Universität, Frankfurt am Main, GERMANY

ABSTRACT

Predictions from the RQMD model are systematically compared to recently published charged hadron distributions of AGS Experiment 802 for central Si+Au collisions at 14.6A GeV/c, taking into account both the experimental trigger condition and acceptance. The main features of the data, including K^+ production, can be understood quantitatively to better than 20% within the framework of the model, although several discrepancies are found, most importantly for the proton spectra.

1. INTRODUCTION

The main purpose of heavy-ion experiments at high energies is to produce and study nuclear matter under unusual conditions, e.g., at high densities and temperatures. Several detailed models of nucleus-nucleus collisions have been developed (see, e.g., Refs. 1-4), all based on a fully confined phase and on conventional particle production mechanisms.

The Relativistic Quantum Molecular Dynamics (RQMD) model[2] produces hadrons through the excitation of baryonic and mesonic resonances. Heavy resonances (more than 2 GeV for baryons and more than 1 GeV for mesons) are treated in the string picture following the Lund model[1] and all particles are allowed to reinteract (baryon-baryon, baryon-meson, and meson-meson). The model provides a complete time-dependent description of the evolution of each event. The probabilities for excitation of specific channels are governed by experimental cross-sections to the extent possible. The formation points of hadrons are taken from the properties of resonance decay and string fragmentation. Previous comparisons of RQMD predictions and AGS heavy ion data may be found in Refs. 5-9. In particular, the RQMD model gives a good account of global observables, such as transverse energy[5] and charged particle multiplicities[6]. Based on the successes with global observables, it is expected that the model should agree with the data at least at the 25% level, where the experimental systematic error for the data used here is 10-15%. This expectation is largely borne out by the present study.

The experimental data in this paper are from BNL-AGS Experiment 802 (E802), a movable single-arm magnetic spectrometer setup[10]. Early E802 data from a run in December 1987 demonstrated a K^+/π^+ ratio of 19±1% for 14.6A GeV/c central Si+Au collisions[11,12], considerably above the p+p ratio of 5-6% (see Ref. 13). The data used in the present comparison are from December 1988 and June 1989, are published in the survey paper of Ref. 14, and encompass protons, pions, and kaons over a broad rapidity range ($0.6 < y < 2.8$ for pions). In this paper we concentrate our attention on the central Si+Au system. What sets the present comparison aside from previous ones (see, e.g., Refs. 4,5) is a systematic approach starting from the trigger conditions and encompassing all the data, including strangeness production, stopping and momentum conservation. Throughout the paper the influence of the experimental acceptances on the model results is given close attention.

2. THE RQMD EVENT SAMPLES AND THE TRIGGER CONDITION

The experimental trigger cross section $\sigma_{trig} = 263$ mb corresponds to about 7% of the total inelastic cross section for Si+Au and is defined by a cut on "apparent" charged multiplicities > 173. The word "apparent" stands for multiplicities in the experimental acceptance, without corrections for gamma conversion to e^+-e^-, multihits and delta electrons. The multiplicity condition was introduced in software[14] and is different from the hardware trigger used earlier[11,12].

The main RQMD sample consists of 1537 events generated by version 1.07 of the code, with impact parameters $0 < b < 4$ fm and a weighting proportional to b, corresponding to a cross section of 503 mb (see Fig. 1, solid histogram.) For reference, the impact parameters $0 < b < 3.4$ fm correspond to a full overlap between projectile and target nuclei in a hard sphere picture. To match the experimental σ_{trig}, 806 events of the RQMD sample were chosen by demanding that $n_{ch} \geq 154$, where n_{ch} is the charged multiplicity from an RQMD event in the ideal experimental acceptance[10] ($6^\circ < \theta < 149^\circ$, where θ is the polar angle from the beam direction, and momentum thresholds $p > 0.30$ GeV/c for protons and $p > 0.05$ GeV/c for pions). The impact parameter distribution of this sample is shown by the broken histogram in Fig. 1. The $n_{ch} \geq 154$ sample encompasses nearly all events with $b < 2$ fm, but also has a significant contribution from $2 < b < 3$ fm. The sensitivity of the RQMD predictions to impact parameter selection was tested and found to be small for events with $b < 4$ fm.

The E802 cut at 7% on apparent charged multiplicity does not correspond to a sharp cut at 7% in real charged multiplicity, as some events with comparatively low charged particle multiplicity and a comparatively high number of delta electrons and gamma-conversion e^+e^- pairs would be accepted by the cut. Monte Carlo simulations of these effects indicate a spread in apparent multiplicity of 5 to 6 units, at the one-sigma level, for events with a fixed real multiplicity. Given the low sensitivity to the n_{ch} cut of the RQMD results, the trigger differences between experiment and model are not of consequence.

Another sample of RQMD events is also used in the comparisons to the data. This sample of 520 events with $0 < b < 2.5$ fm was calculated with the attractive part of the quasi-potentials acting between baryon resonances modified as explained in Ref. 5, i.e., with the delta-delta and nucleon-baryon attractions turned off. This sample is referred to below as the RQMD2 sample. No n_{ch} filter was set since more than 95% of the events satisfied the $n_{ch} \geq 154$ criterion.

3. SPECTRA AND RAPIDITY DISTRIBUTIONS

Spectra in the form of the invariant cross section normalized per event versus $m_t - m$ (where $m_t = \sqrt{p_t^2 + m^2}$, $p_t = p \sin\theta$, where p is the momentum and m the rest mass) were constructed from the RQMD events for protons, $\pi^{\pm}$ and $\mathrm{K}^{\pm}$. Each spectrum was fit to an exponential with the maximum likelihood procedure for Poisson statistics within the experimental $m_t - m$ acceptance for rapidity bins of $\Delta y = 0.3$, (0.5 for K^-):

$$\frac{1}{N_{trig}} \left(E \frac{d^3n}{dp^3} \right) = A \exp(-(m_t - m)/B) \quad , \tag{1}$$

where N_{trig}=the number of events in the sample=806 for the present RQMD set, and A and B are fit parameters, with B called the inverse slope parameter. The integral of multiplicity density (per event), dn/dy, was evaluated as

$$dn/dy = \int_0^{2\pi} d\phi \int_m^{\infty} A \exp(-(m_t - m)/B) m_t dm_t = 2\pi A(B^2 + mB) \quad . \tag{2}$$

The distribution dn/dy can also be found directly by counting the number of RQMD particles in each rapidity interval.

3.1. Acceptance

The RQMD hyperons and K_s^0 were decayed immediately after the collision and thus no account was taken for the variation of the experimental acceptance with the position of the decay vertex. In E802 only tracks that point back to the target are accepted: this is defined by a ± 3 cm cut in the x and y directions, where the (x,y) plane is defined as a plane perpendicular to the beam direction (z-axis) with its origin at the target center

(z=0) (see Ref. 14.) For the hyperons, the decay protons will largely be counted, but the decay pions will not. The overwhelming part of these pions will have m_t values below the E802 m_t acceptance, so the effect for the comparisons presented here is very small. For the K^0_s, it is evaluated that about 5% of the decay pions will not be accepted by E802, so the RQMD estimates made here within the E802 acceptance overcount the $\pi^{\pm}$ by less than 2%.

3.2. Protons

Figure 2 shows a comparison of RQMD proton spectra at $y = 0.7$ and $y = 1.90$ to E802 spectra at the same rapidities. (Note that the $y = 1.90$ spectra have been multiplied by 0.01 for display reasons.) At both rapidities the RQMD spectra fall off more steeply with m_t than do the experimental spectra; i.e., $B_{RQMD} < B_{E802}$. This is a general feature in the total experimental rapidity acceptance $0.4 < y < 2.2$. The dn/dy as obtained via Eqs. (1) and (2) are shown in Fig. 3, where RQMD fits in the E802 acceptance are shown as open squares. The RQMD model does not produce clusters (d, t, ^{3}He, etc.), so it is reasonable to add the measured deuterons, which contribute most of these clusters, to the measured protons for the comparison. The filled octagons show the p+d results from E802, when p and d multiplicities are added at the same rapidity. Statistical uncertainties are shown only when they are larger than the size of the symbol. The shapes of the two dn/dy distributions are different: RQMD is convex and E802 is concave. For $0.75 < y < 2.0$ the RQMD points are above the experimental points.

Figure 3 also shows the E802 proton and deuteron results from a 2% cut on apparent multiplicity (black squares). This cut corresponds to the centrality cut used in Experiment E814 (Ref. 15), and represents the most central cut reasonable within the statistics of E802. The RQMD points are still above the data for the midrapidity region, $1.0 < y < 2.0$.

The slopes, B, of the RQMD proton spectra depend on the quasi-potentials acting between the baryon resonances used in the calculations (see Ref. 5.) The calculation which produced the RQMD2 sample (the same calculation described in Ref. 5), yields

larger inverse slope parameters, i.e., a less steep fall-off with $m_t - m$. Figure 4 shows a comparison of the B-values obtained from fitting proton spectra in the E802 experimental $m_t - m$ acceptance. The black squares are from the experiment, the open squares show the results from the standard RQMD calculations (no error bars shown), while the open octagons are from the calculations with modified potentials (RQMD2). The standard RQMD always underpredicts the observed B-values, while the RQMD2 does better at low rapidities, but also underpredicts B significantly for $y > 1.2$. Addition of the E-802 deuteron spectra to the proton spectra (at 1/2 the deuteron $m_t - m$ values) makes no change in this result. The dn/dy values for RQMD and RQMD2 agree well with one another for $y \geq$1.0, while RQMD2 is 10 to 20% above the RQMD values for y=0.45 and 0.75. The measured slope parameters for the 2% and 7% cuts agree with one another, and the peaking of the B-values at $y = 1.5$ seen in Fig. 4 is repeated for the 2% cut.

The model has too many protons in midrapidity (Fig. 3), for which there are two possible causes: the first is too much "stopping", i.e., the interactions slow down the protons too much while creating too many pions (see below.) The second possible cause is an excessive conversion of neutrons to protons from an overly rapid chemical equilibration, an effect that will cause an overproduction of π^- relative to π^+, as is also observed (see below.) Indeed, RQMD predicts a neutron/proton ratio of very nearly n/p=1.0 for rapidities, $y \geq 1.0$, indicating a high degree of proton-neutron equilibration in the model.

3.3. Pions

The π^+ spectra for $y = 1.10$ and 2.50 are shown in Fig. 5. The agreement between experiment (black squares) and theory (open squares) is good. Close examination of the RQMD pion spectra reveals that they are in general not exponential; they often exhibit a steep rise at low $m_t - m$ (see, e.g., the spectrum for $y = 1.10$).

The spectra may be fitted to a single exponential within the experimental $m_t - m$ acceptance with χ^2 values per degree of freedom around 1-1.5, and the slope parameters for theory and experiment agreeing well. The resulting dn/dy values are shown in Fig. 6a,

for both π^+ and π^- and with the π^- values multiplied by 0.1 for display purposes. The RQMD dn/dy are generally higher than the experimental values by ≈10% for π^+ and ≈15% for π^-. The distribution shapes are very similar.

The π^+ dn/dy values for the 2% multiplicity cut (not shown) give quantitative agreement with RQMD for $1.0 \leq y \leq 2.0$, while there is still a small discrepancy at the outer ranges of the rapidity interval. RQMD2 gives a pion yield close to RQMD. The model acts as a somewhat more central event sample than the 7% cross section cut would indicate, a trend that is not inconsistent with the proton discussion above.

The RQMD pion spectra in the full $m_t - m$ acceptance require a sum of two exponentials to be adequately fit, where one component has a B value near 80 MeV and the other has $B \approx 150$ MeV. In cases like this, the total dn/dy evaluated from a fit in the experimental acceptance and from counting in the full acceptance are of course quite different, as demonstrated in Fig. 6b for π^+. The RQMD model shows that the steep low-p_t part of the pion spectra (which is outside the E802 acceptance) originates predominantly from decays of Δ-resonances[8,16]. (Λ decays do not contribute to the π^+ spectrum, but are important for π^-.) The low p_t rise for pions, predicted by RQMD, has been observed in AGS experiments E810[17] and E814[18].

3.4. Kaons

The agreement between data and theory for kaons is of similar quality as for pions. This is reflected in the dn/dy integrals shown in Fig. 7 for both K^+ and K^-. On the average the E802 K^+ dn/dy are ≈20% higher than the RQMD values, while the K^- measurements are ≈20% lower than the theory. The distribution shapes agree well. The experimental values of the slope parameter, B for K^+ are larger than the RQMD predictions, typically ≈220 MeV vs. ≈180 MeV.

The conventional ratios K^+/π^+ and K^+/K^- are displayed in Fig. 8 versus rapidity for both E802 and RQMD. The experimental K^+/π^+ ratio is consistently higher than the

RQMD ratio, an effect that is not due to the low-p_t rise in the RQMD π^+ spectra, as all fits were made in the E802 acceptance. Also the K^+/K^- ratios are different, with the E802 ratio being consistently higher. The 2% centrality cut for E802 does not change any of the ratios discussed, so it is unlikely that the discrepancy is caused by differences in the trigger conditions. In the RQMD model there are substantial contributions to the K^+ and K^- production from baryon-meson interactions and some contribution to K^- from meson-meson interactions[6]. These cascade-like interactions depend strongly on the dynamics of the nuclear collisions, and it is unlikely that a somewhat schematic model such as RQMD should describe this complex situation entirely accurately. The deviations are emphasized in the ratios shown.

4. AVERAGE MULTIPLICITIES AND MOMENTUM SUMS

Table 1 shows the multiplicities for protons, pions and kaons summed over the E802 rapidity acceptance. The deuteron multiplicities have been added to the proton multiplicities for E802. The ratios of E802/RQMD multiplicities in the last column show that the RQMD model overpredicts the particle yield by about 25% on the average. For K^+ the model underpredicts by a similar amount.

Both π^+ and π^- have been measured in identical rapidity intervals, so the particle ratio $R(\pi) = \Delta n(\pi^-)/\Delta n(\pi^+)$ is of relevance. Because of the neutron surplus in the Au target, it is expected that the ratio should be larger than unity. Table 1 yields $R(\pi)$=1.09±0.02 for E802 and 1.15±0.01 for RQMD. The difference in the E802 and RQMD ratios is near three standard deviations and may be significant. (See also the discussion in Sect. 3.3.)

The total transverse momentum production shown in Table 2 was calculated from the exponential fits (Eq. 1) in the E802 $m_t - m$ interval by:

$$P_t = \sum_{y_1}^{y_2} \langle p_t \rangle \left(\frac{dn}{dy} \right) \Delta y \quad , \tag{3}$$

where y_1 and y_2 are the rapidity limits given in the table, Δy is the bin size, and

$$\langle p_t \rangle = \frac{1}{dn/dy} \int_0^{2\pi} d\phi \int_m^{\infty} A \exp(-(m_t - m)/B)\ m_t \sqrt{m_t^2 - m^2}\ dm_t \tag{4}$$

$$= \frac{m^2}{B+m}\ \exp(m/B)\ K_2(m/B) \quad ,$$

where K_2 is a modified Bessel function of second order.

The total longitudinal momemtum, $P_\parallel$, is defined as

$$P_\parallel = \sum_{y_1}^{y_2} \langle p_\parallel \rangle \left(\frac{dn}{dy} \right) \Delta y \tag{5}$$

with

$$\langle p_\parallel \rangle = \langle m_t \rangle \sinh y = \frac{1}{dn/dy} \int_0^{2\pi} d\phi \int_m^{\infty} A \exp(-(m_t - m)/B)\ m_t^2\ \sinh y\ dm_t$$

$$= \sinh y \cdot 2B \cdot \frac{1 + m/B + m^2/2B^2}{1 + m/B} \quad . \tag{6}$$

For protons (with deuterons added for E802), the P_t ratio E802/RQMD is 0.96, compared with 0.84 for $P_\parallel$ and 0.73 for the multiplicities, Δn. The experiment clearly has larger $\langle p_t \rangle$ and $\langle p_\parallel \rangle$ values than RQMD. This is reversed for the pions, for which the E802/RQMD ratio is smaller for the momenta than for the multiplicities, although the effect is relatively smaller than for the protons. The K^+ trend is like that for the protons. This analysis supports the discussion given in the above sections.

$P_\parallel$ is a conserved quantity, so the less than unity ratio in Table 2 for "All" indicates that the E802/RQMD ratio at rapidities higher than those covered by the E802 acceptance — higher rapidities rather than lower because of the $\sinh(y)$ weighting in Eq. 6 — should be going from below one to above one. This conclusion is similar to the one drawn from other model comparisons in Ref. 19, except that the E802 deficit is much smaller in the present comparison.

5 CONCLUSIONS

The overall agreement between the RQMD model and the E802 experimental data is quite satisfactory, mostly within ≈20%. (Recall that there is a 10-15% systematic error associated with the experimental results[14].) The largest differences between RQMD and E802 occur for the proton dn/dy distributions (Fig. 3) and for the proton inverse slope parameter distributions (Fig. 4).

It is our conclusion that the calculation gives too many protons in the central rapidity region as compared to the E802 data. The relevant processes for this disagreement are a difference in the baryon stopping power, and too strong of a removal of the initial target neutron excess. A contribution from the latter process receives support from the excess of negative mesons over positive mesons predicted by the model and not observed experimentally; also predicted is a neutron/proton ratio near 1.0 for $y \geq 1.0$.

The further discrepency, the higher average p_t around midrapidity, is just the reflection of the larger experimental proton slope parameters as discussed above. While the density dependence of the quasipotentials can be successfully manipulated to harden the proton slopes in the center of the participant fireball ($y \in (1, 1.2)$), it does not give sufficient repulsion for the protons forward of rapidity 1.2. This may point towards an additional repulsion due to the momentum dependence of nuclear mean fields in dense matter. It is well known that such a momentum dependence is present at ground-state density which is experimentally accessible via optical potential measurements in p+A reactions. However, no safe knowledge exists on how the density and momentum dependence of mean fields are intertwined.

The large experimentally observed splitting between the proton and the pion slope parameters — which is qualitatively confirmed by RQMD and even somewhat underestimated in the forward rapidity region — is rather remarkable, and may point towards the importance of collective flow in nucleus-nucleus reactions at AGS energy. The collective flow component of the transverse momenta increases with the mass of a particle. In RQMD

this is the most important mechanism which leads to a slope parameter splitting for the various hadron species.

In general, the RQMD model seems to describe reasonably well the mechanism of heavy ion reactions at AGS energies. The hadron distributions from central nucleus-nucleus collisions can not be explained by simple superpositions of nucleon-nucleon collisions. The comparison of the data with the predictions of the transport model shows clearly that the rescattering of produced particles in the hadronic matter plays a major role in the evolution of the collisions. In particular, the production and rescattering of hadron resonances are the key processes to understanding the stopping power, transverse mass spectra and strangeness enhancement observed experimentally.

ACKNOWLEDGEMENTS

This work has been supported in part by the U.S. Department of Energy under contracts with Brookhaven National Laboratory and Los Alamos National Laboratory. R. Mattiello wishes to express his gratitude to Drs. W. Greiner and H. Stöcker for providing excellent working conditions and for many helpful discussions.

REFERENCES

a) Now at LPNHE-Ecole Polytechnique, F-91178 Palaiseau, France.

b) Now at the Niels Bohr Institute for Astronomy, Physics and Geophysics, DK-2100 Copenhagen Ø, Denmark.

c) Now at the Institut für Theoretische Physik, Johann Wolfgang Goethe Universität, Frankfurt am Main, Germany.

1) B. Nilsson-Almqvist and E. Stenlund, Computer Phys. Comm. **43**, 387 (1987); B. Andersson, G. Gustafson and B. Nilsson-Almqvist, Nucl. Phys. **B281**, 289 (1987).

2) H. Sorge, H. Stöcker and W. Greiner, Ann. Phys. (NY) **192**, 266 (1989); Nucl. Phys. **A498**, 567c (1989); Z. Phys. **C47**, 629 (1990).

3) K. Werner, Z. Phys. **C42**, 85 (1989).

4) Y. Pang, T.J. Schlagel and S. Kahana, Phys. Rev. Lett. **68**, 2743 (1992).

5) H. Sorge, R. Mattiello, H. Stöcker and W. Greiner, Phys. Rev. Lett. **68**, 286 (1992).

6) R. Mattiello, H. Sorge, H. Stöcker and W. Greiner, Phys. Rev. Lett. **63**, 1459 (1989).

7) H. Sorge, A. von Keitz, R. Mattiello, H. Stöcker and W. Greiner, Phys. Lett. **B243**, 7 (1990).

8) H. Sorge, R. Mattiello, A. Jahns and W. Greiner, Phys. Lett. **B271**, 37 (1991).

9) A. Jahns, H. Stöcker, W. Greiner and H. Sorge, Phys. Rev. Lett. **68**, 2895 (1992).

10) T. Abbott *et al.*, The E802 Collaboration, Nucl. Instrum. and Methods **A290**, 41

(1990).

11) T. Abbott *et al.*, The E802 Collaboration, Phys. Rev. Lett. **64**, 847 (1990).

12) T. Abbott *et al.*, The E802 Collaboration, Phys. Rev. Lett. **66**, 1567 (1991).

13) J.V. Allaby *et al.*, CERN Report No. 70-12, 1970 (unpublished); H. Bøggild *et al.*, Nucl. Phys. **B57**, 77 (1973); D. Dekkers *et al.*, Phys. Rev. **137**, B962 (1965); U. Becker *et al.*, Phys. Rev. Lett. **37**, 1731 (1976).

14) T. Abbott *et al.*, The E802 Collaboration, Phys. Rev. **C50**, 1024 (1994).

15) P. Braun-Munzinger, The E814 Collaboration, Nucl. Phys. **A544**, 137c (1992).

16) H. Sorge, Phys. Rev. **C49**, R1253 (1994).

17) S. Ahmad *et al.*, The E810 Collaboration, Phys. Lett. **B281**, 29 (1992).

18) T. Hemmick, The E814 Collaboration, Nucl. Phys. **A566**, 435c (1994).

19) S. Chapman and M. Gyulassy, Phys. Rev. Lett. **67**, 1210 (1991).

Table 1

Average multiplicities

Particle	Rapidities	Δn(RQMD)	Δn(E802)	E802/RQMD
p (+d)	0.4-2.2	45.2±0.2	33.0±0.2	0.73±0.01
π^+	0.6-2.8	32.4±0.2	27.0±0.3	0.83±0.01
π^-	0.6-2.8	37.3±0.3	29.5±0.3	0.79±0.01
K^+	0.6-2.2	3.5±0.1	4.3±0.1	1.22±0.05
K^-	0.7-2.3	1.03±0.04	0.90±0.06	0.87±0.07
All		119.4±0.4	94.7±0.5	0.79±0.01

Table 2

Momentum Sums

Part.	Rapidities	P_t GeV/c		$P_\parallel$ GeV/c		E802/RQMD	
		E802	RQMD	E802	RQMD	P_t	$P_\parallel$
p	0.4-2.2	23.7±0.2	26.1±0.2	63.1±0.3	78.3±0.6	0.91±0.01	0.81±0.01
d	0.4-1.6	2.6±0.1		5.7±0.1			
p+d						0.96±0.01*	0.84±0.01*
π^+	0.6-2.8	9.2±0.1	11.8±0.1	26.4±0.2	33.8±0.3	0.78±0.01	0.78±0.01
π^-	0.6-2.8	9.9±0.1	13.5±0.1	28.1±0.2	38.3±0.4	0.73±0.01	0.73±0.01
K^+	0.6-2.2	2.3±0.1	1.63±0.05	6.4±0.2	4.9±0.1	1.4±0.1	1.3±0.1
K^-	0.7-2.3	0.46±0.05	0.52±0.03	1.2±0.1	1.7±0.1	0.88±0.11	0.71±0.07
All*		46.9±0.3	53.6±0.3	128.1±0.5	157.0±0.8	0.88±0.01	0.82±0.05

* Deuterons added to the E802 value with 50% of the quoted momentum value.

Figure Captions

Fig. 1 The impact parameter distributions for the entire RQMD event sample (1537 events, fully drawn histogram) and the "central" sample (806 events, broken histogram). The central distribution was obtained by setting conditions on proton and pion momenta and the charged multiplicity in the acceptance of the E802 multiplicity detector (see the text for details).

Fig. 2 Comparison of proton spectra from E802 (filled squares) and RQMD (open squares). The invariant cross-section per event is plotted versus transverse kinetic energy $m_t - m$, for two different rapidity intervals y=0.70 and y=1.90. For E802 the interval width is Δy=0.2, while it is 0.3 for RQMD. The error bars are statistical, assuming a Poisson distribution. The y=1.90 cross sections have been multiplied by 0.01 for reasons of display.

Fig. 3 Proton rapidity distributions dn/dy. The open squares denote the multiplicities per unit rapidity obtained by integration of the RQMD proton spectra within the E802 m_t acceptance. Black octagons denote the E802 dn/dy, where the deuteron yield has been added to the proton dn/dy at the same rapidity. Black squares are $p + d$ E802 dn/dy for a more central multiplicity cut, 2% of σ_{inel} instead of the standard 7%.

Fig. 4 Inverse slope parameters B (in GeV), as defined in Eq. (1), plotted versus rapidity for protons. Black squares denote E802 data, open squares RQMD results in the E802 acceptance and finally open octagons stand for RQMD2 results in the experimental acceptance.

Fig. 5 Spectra for π^+ in the two rapidity intervals y=1.10 and y=2.50. Open squares are from RQMD, while black squares are from E802. The y=2.50 invariant cross sections have been multiplied by 0.01 for reasons of display. The rapidity range is Δy=0.2 for E802 and 0.3 for RQMD. Error bars are statistical only.

Fig. 6 a) Rapidity distributions dn/dy for π^+ (squares) and π^- (octagons) from E802 (black symbols) and RQMD analyzed in the experimental acceptance (open symbols). The π^- dn/dy have been divided by 10 for reasons of display. b) Comparison between dn/dy for π^+ from RQMD from in two different $m_t - m$ acceptances. The black points are from single exponential fits in the E802 acceptance, while the open points were obtained by counting over the entire $m_t - m$ range.

Fig. 7 Rapidity distributions dn/dy for K^+ (squares) and K^- (octagons) from E802 (black symbols) and RQMD analyzed in the experimental acceptance (open symbols).

Fig. 8 Comparison of multiplicity ratios from E802 (black symbols) and RQMD analyzed in the experimental acceptance (open symbols). The upper frame gives the $\Delta n(K^+)/\Delta n(K^-)$ ratio plotted against laboratory rapidity, while the lower frame shows the ratio $\Delta n(K^+)/\Delta n(\pi^+)$.

This figure "fig1-1.png" is available in "png" format from:

http://arXiv.org/ps/nucl-th/9412009v1

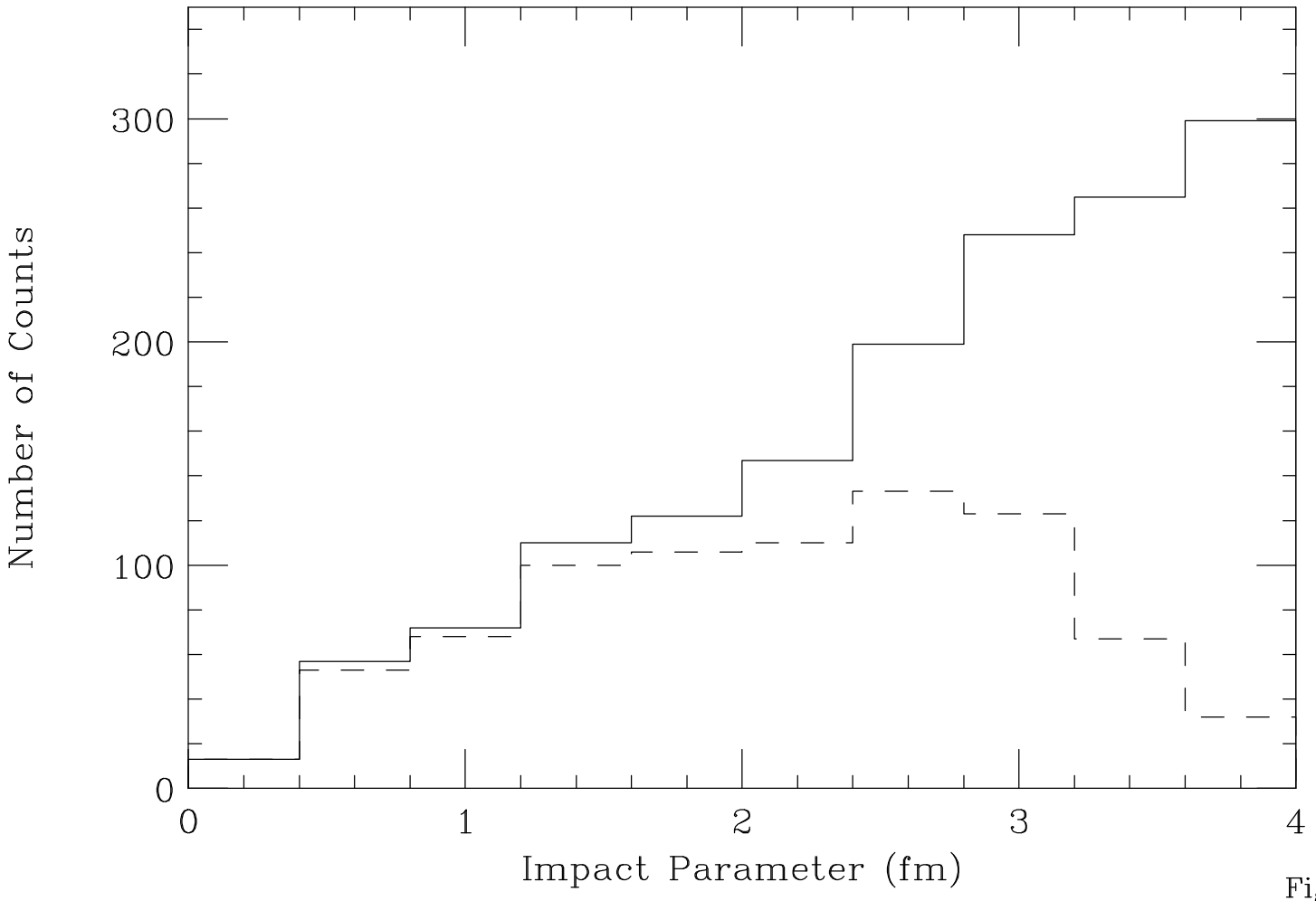

Fig. 1

This figure "fig2-1.png" is available in "png" format from:

http://arXiv.org/ps/nucl-th/9412009v1

This figure "fig1-2.png" is available in "png" format from:

http://arXiv.org/ps/nucl-th/9412009v1

This figure "fig2-2.png" is available in "png" format from:

http://arXiv.org/ps/nucl-th/9412009v1

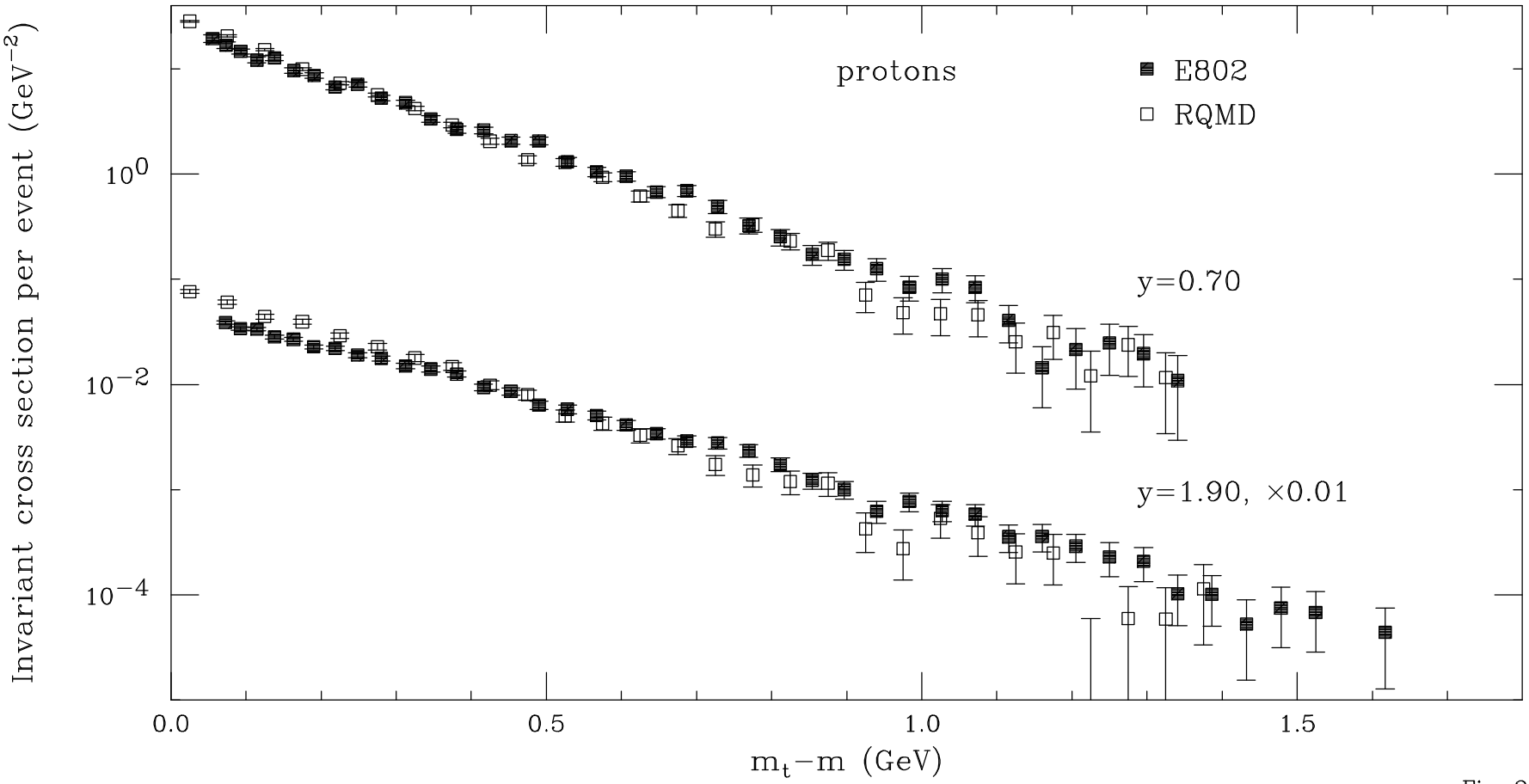
protons
E802
RQMD
y=0.70
y=1.90, ×0.01
Invariant cross section per event (GeV^{-2})
10^{0}
10^{-2}
10^{-4}
0.0
0.5
1.0
1.5
$m_t - m$ (GeV)

Fig. 2

This figure "fig1-3.png" is available in "png" format from:

http://arXiv.org/ps/nucl-th/9412009v1

This figure "fig2-3.png" is available in "png" format from:

http://arXiv.org/ps/nucl-th/9412009v1

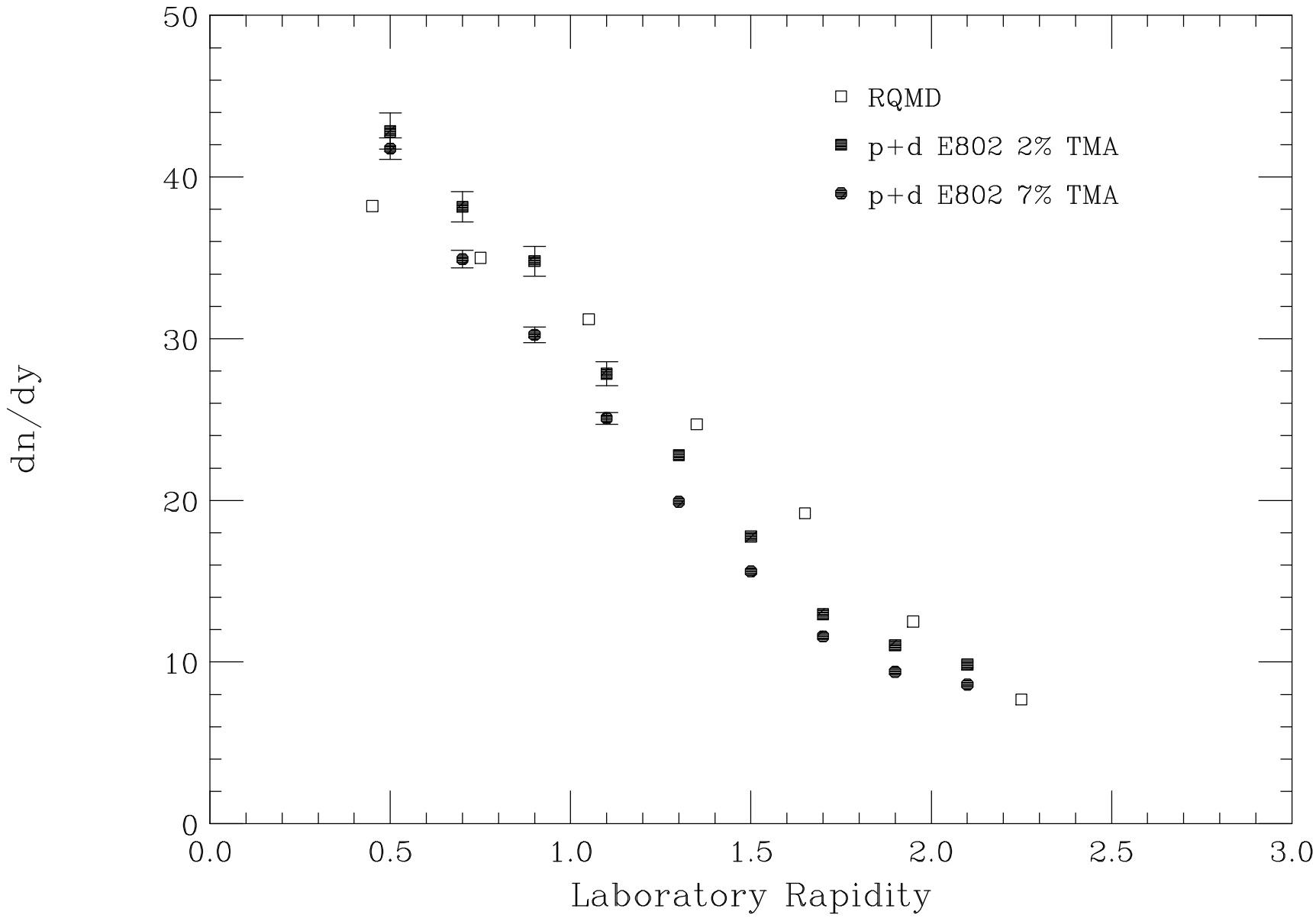
RQMD
p+d E802 2% TMA
p+d E802 7% TMA
dn/dy
Laboratory Rapidity
0
10
20
30
40
50
0.0
0.5
1.0
1.5
2.0
2.5
3.0

Fig. 3

This figure "fig1-4.png" is available in "png" format from:

http://arXiv.org/ps/nucl-th/9412009v1

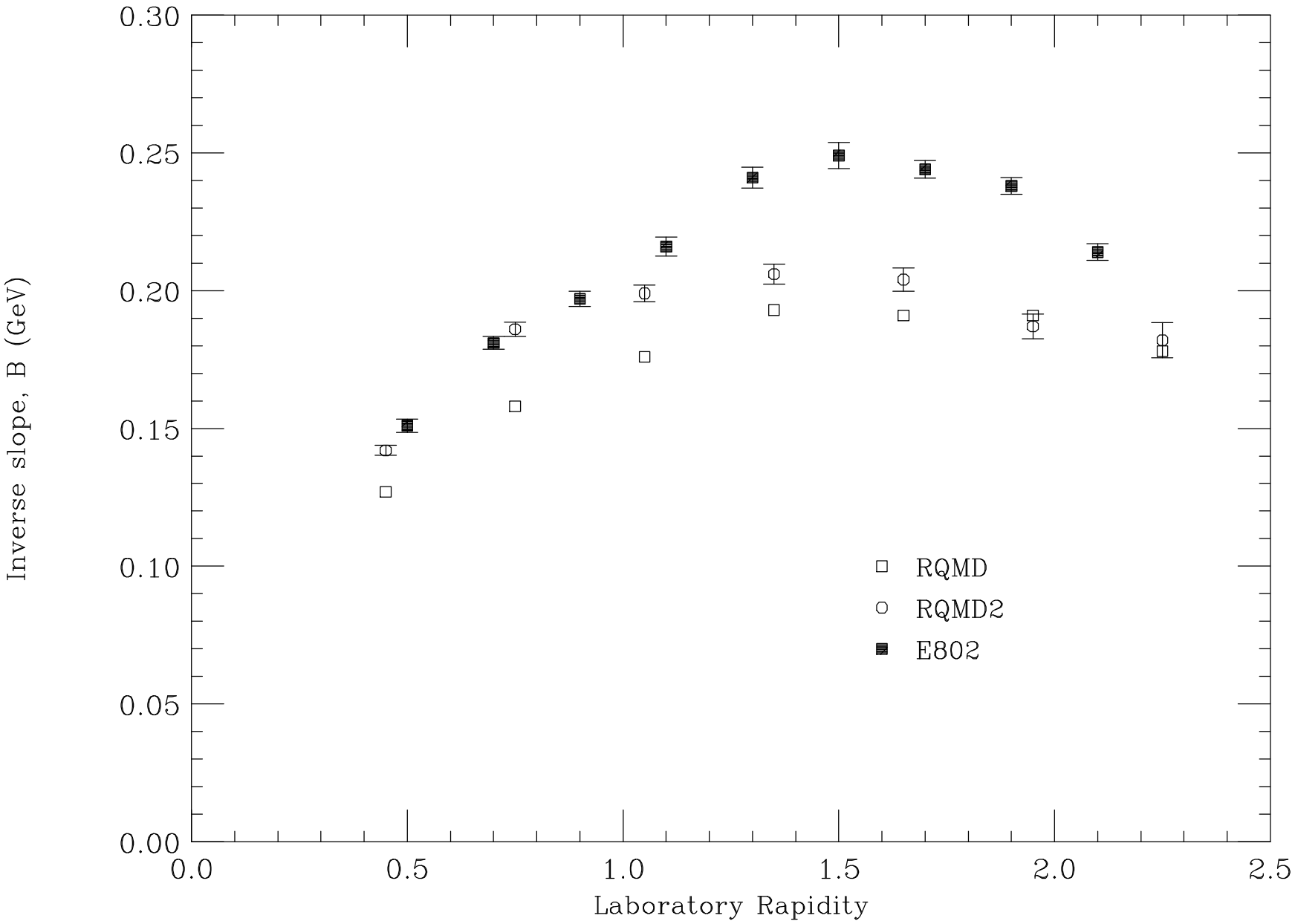
0.30
0.25
0.20
0.15
0.10
0.05
0.00
Inverse slope, B (GeV)
0.0
0.5
1.0
1.5
2.0
2.5
Laboratory Rapidity
RQMD
RQMD2
E802

Fig. 4

This figure "fig1-5.png" is available in "png" format from:

http://arXiv.org/ps/nucl-th/9412009v1

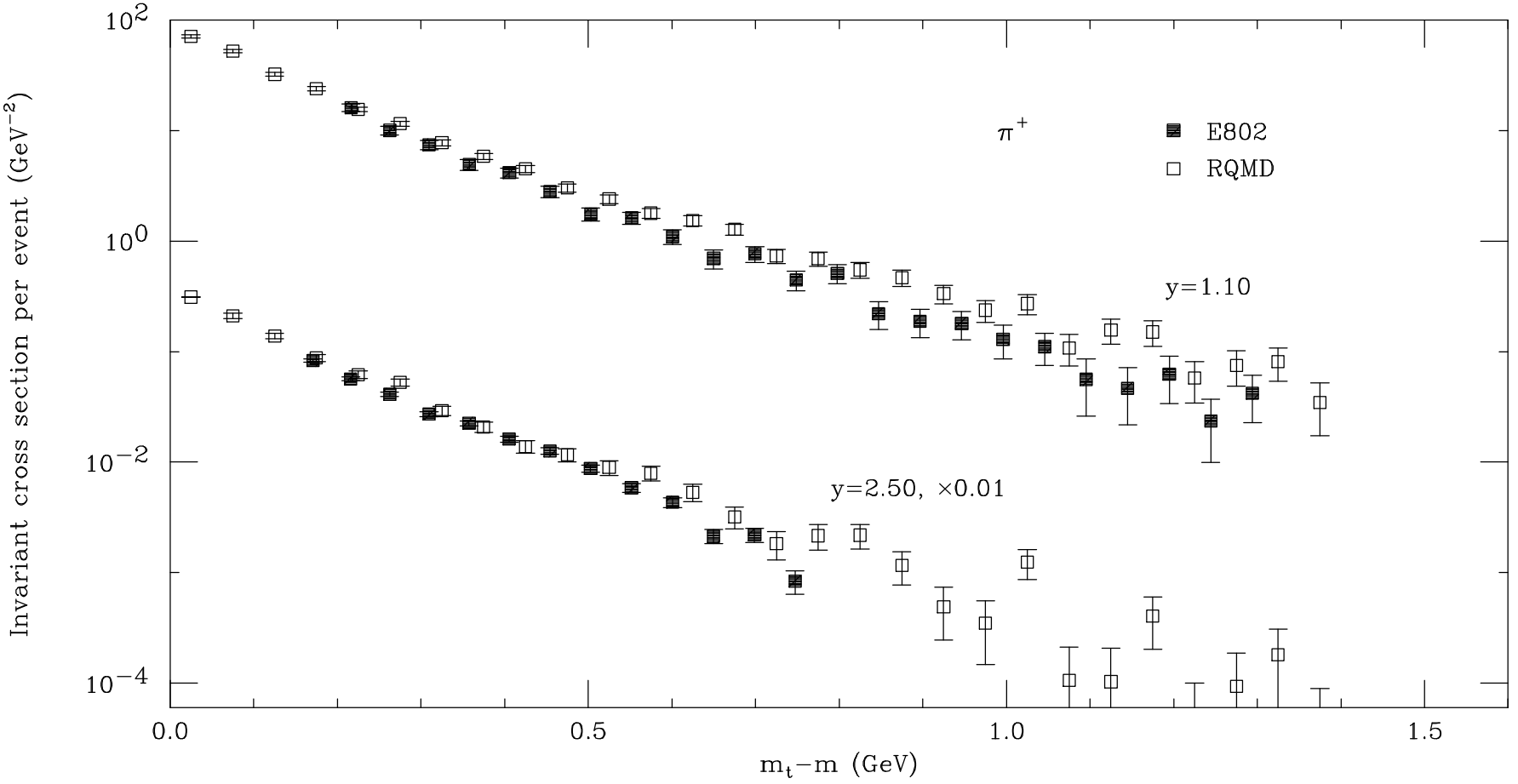
Invariant cross section per event (GeV^{-2})
10^2
10^0
10^{-2}
10^{-4}
0.0
0.5
1.0
1.5
$m_t - m$ (GeV)
π^+
E802
RQMD
y=1.10
y=2.50, ×0.01

Fig. 5

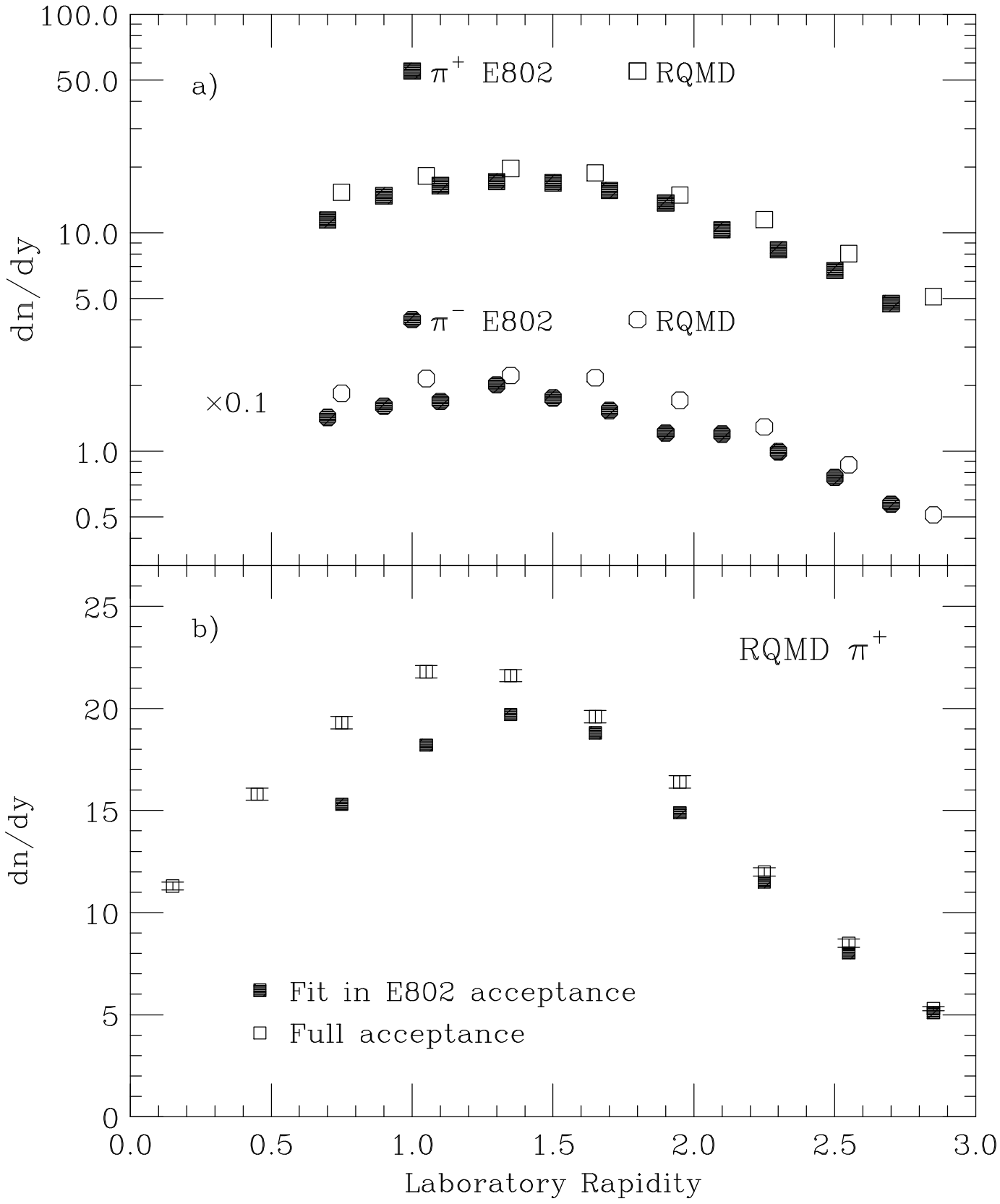
a)
π^+ E802
RQMD
π^- E802
RQMD
×0.1
dn/dy
100.0
50.0
10.0
5.0
1.0
0.5
b)
RQMD π^+
Fit in E802 acceptance
Full acceptance
dn/dy
25
20
15
10
5
0
0.0
0.5
1.0
1.5
2.0
2.5
3.0
Laboratory Rapidity

Fig. 6

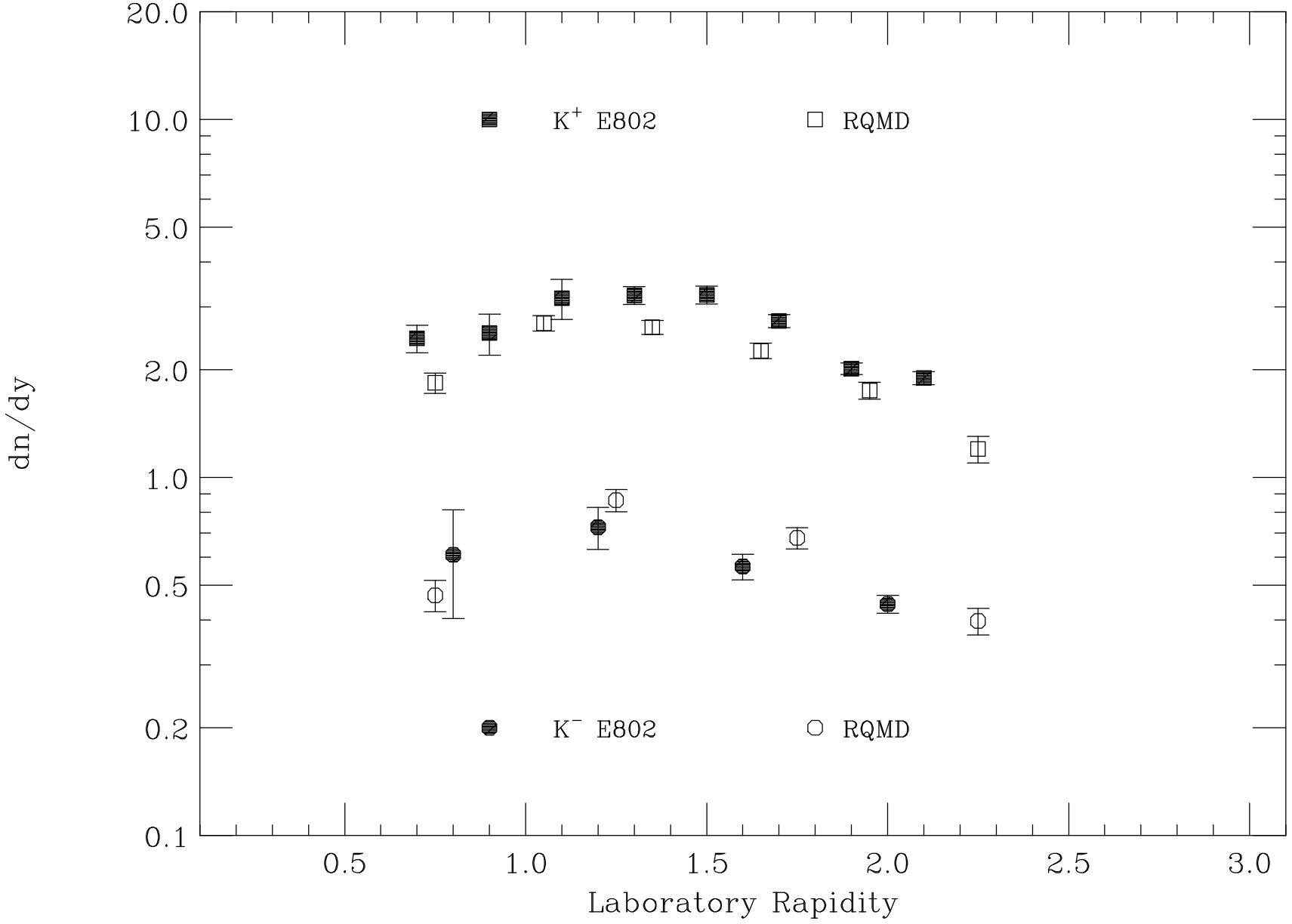
20.0
10.0
5.0
2.0
1.0
0.5
0.2
0.1
dn/dy
K+ E802
RQMD
K− E802
RQMD
0.5
1.0
1.5
2.0
2.5
3.0
Laboratory Rapidity

Fig. 7

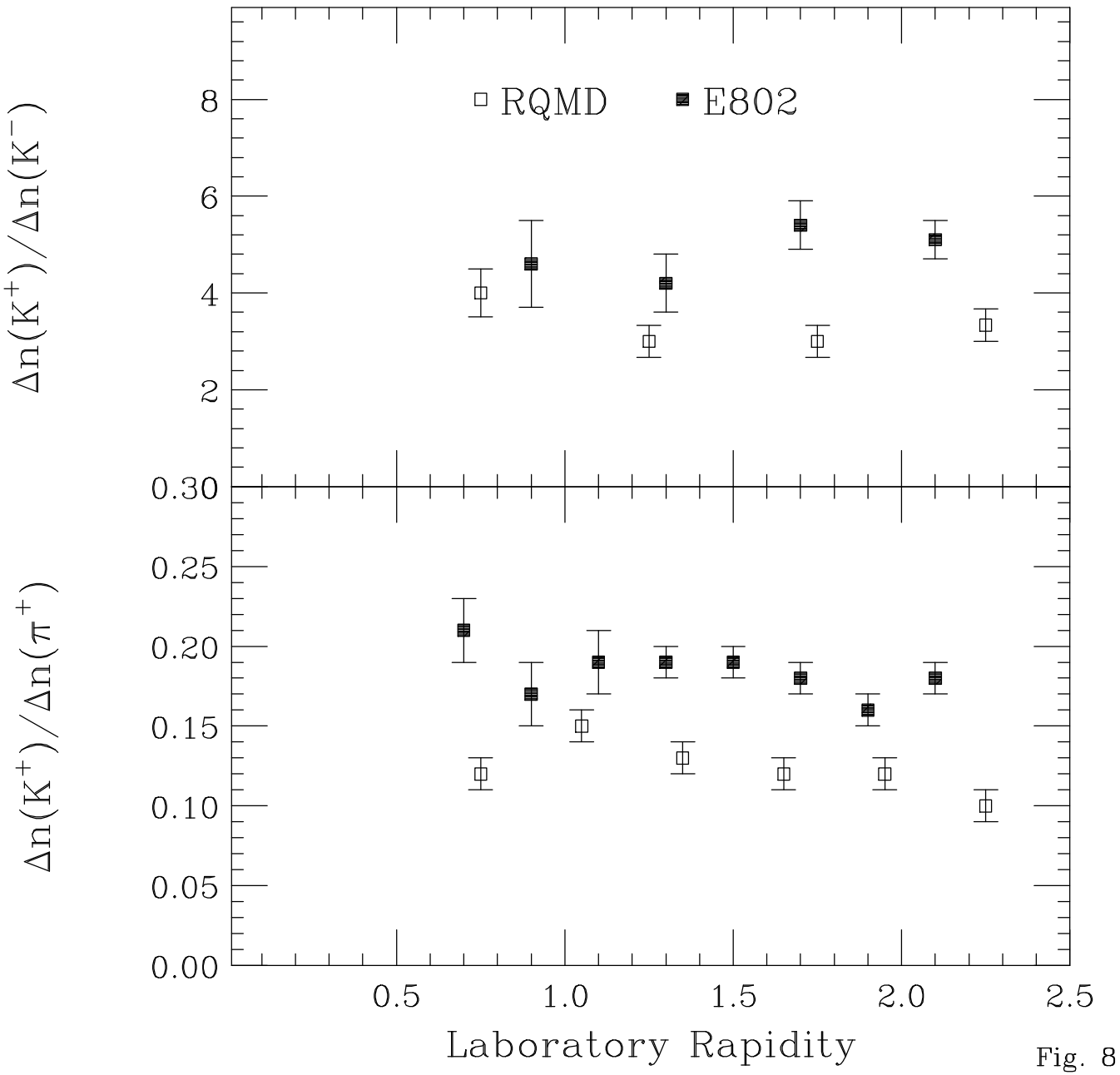
RQMD
E802
$\Delta n(K^+)/\Delta n(K^-)$
$\Delta n(K^+)/\Delta n(\pi^+)$
Laboratory Rapidity
0.5
1.0
1.5
2.0
2.5
0.00
0.05
0.10
0.15
0.20
0.25
0.30
2
4
6
8

Fig. 8